

## VUV photoionization and dissociative photoionization of the prebiotic molecule acetyl cyanide: Theory and experiment

A. Bellili, M. Schwell, Y. Bénilan, N. Fray, M.-C. Gazeau, M. Mogren Al-Mogren, J.-C. Guillemin, L. Poisson, and M. Hochlaf

Citation: *The Journal of Chemical Physics* **141**, 134311 (2014); doi: 10.1063/1.4896987

View online: <http://dx.doi.org/10.1063/1.4896987>

View Table of Contents: <http://scitation.aip.org/content/aip/journal/jcp/141/13?ver=pdfcov>

Published by the [AIP Publishing](#)

---

### Articles you may be interested in

Dissociation of internal energy-selected methyl bromide ion revealed from threshold photoelectron-photoion coincidence velocity imaging

*J. Chem. Phys.* **140**, 044312 (2014); 10.1063/1.4862686

Communication: A vibrational study of propargyl cation using the vacuum ultraviolet laser velocity-map imaging photoelectron method

*J. Chem. Phys.* **137**, 161101 (2012); 10.1063/1.4764306

Zero kinetic energy photoelectron spectroscopy of tryptamine and the dissociation pathway of the singly hydrated cation cluster

*J. Chem. Phys.* **137**, 104312 (2012); 10.1063/1.4752080

Photoelectron spectroscopic study of the Ee Jahn–Teller effect in the presence of a tunable spin–orbit interaction. I. Photoionization dynamics of methyl iodide and rotational fine structure of CH<sub>3</sub>I<sup>+</sup> and CD<sub>3</sub>I<sup>+</sup>

*J. Chem. Phys.* **134**, 054308 (2011); 10.1063/1.3547548

Photoionization-induced dynamics of ammonia: Ab initio potential energy surfaces and time-dependent wave packet calculations for the ammonia cation

*J. Chem. Phys.* **124**, 214306 (2006); 10.1063/1.2202316

---



**AIP** | Chaos

**CALL FOR APPLICANTS**

Seeking new Editor-in-Chief

# VUV photoionization and dissociative photoionization of the prebiotic molecule acetyl cyanide: Theory and experiment

A. Bellili,<sup>1</sup> M. Schwell,<sup>2,a)</sup> Y. Bénilan,<sup>2</sup> N. Fray,<sup>2</sup> M.-C. Gazeau,<sup>2</sup> M. Mogren Al-Mogren,<sup>3</sup> J.-C. Guillemin,<sup>4</sup> L. Poisson,<sup>5</sup> and M. Hochlaf<sup>1,a)</sup>

<sup>1</sup>Laboratoire Modélisation et Simulation Multi Echelle, MSME UMR 8208 CNRS, Université Paris-Est, 5 bd Descartes, 77454 Marne-la-Vallée, France

<sup>2</sup>Laboratoire Interuniversitaire des Systèmes Atmosphériques (LISA), UMR 7583 CNRS, Institut Pierre et Simon Laplace, Universités Paris-Est Créteil et Paris Diderot, 61 Avenue du Général de Gaulle, 94010 Créteil, France

<sup>3</sup>Chemistry Department, Faculty of Science, King Saud University, P.O. Box 2455, Riyadh 11451, Kingdom of Saudi Arabia

<sup>4</sup>Institut des Sciences Chimiques de Rennes, Ecole Nationale Supérieure de Chimie de Rennes, CNRS, UMR 6226, Allée de Beaulieu, CS 50837, 35708 Rennes Cedex 7, France

<sup>5</sup>Laboratoire Francis Perrin, CNRS URA 2453, CEA, IRAMIS, Laboratoire Interactions Dynamique et Lasers, Bât 522, F-91191 Gif/Yvette, France

(Received 7 August 2014; accepted 22 September 2014; published online 7 October 2014)

The present combined theoretical and experimental investigation concerns the single photoionization of gas-phase acetyl cyanide and the fragmentation pathways of the resulting cation. Acetyl cyanide (AC) is inspired from both the chemistry of cyanoacetylene and the Strecker reaction which are thought to be at the origin of medium sized prebiotic molecules in the interstellar medium. AC can be formed by reaction from cyanoacetylene and water but also from acetaldehyde and HCN or the corresponding radicals. In view of the interpretation of vacuum ultraviolet (VUV) experimental data obtained using synchrotron radiation, we explored the ground potential energy surface (PES) of acetyl cyanide and of its cation using standard and recently implemented explicitly correlated methodologies. Our PES covers the regions of tautomerism (between keto and enol forms) and of the lowest fragmentation channels. This allowed us to deduce accurate thermochemical data for this astrobiologically relevant molecule. Unimolecular decomposition of the AC cation turns out to be very complex. The implications for the evolution of prebiotic molecules under VUV irradiation are discussed. © 2014 AIP Publishing LLC. [<http://dx.doi.org/10.1063/1.4896987>]

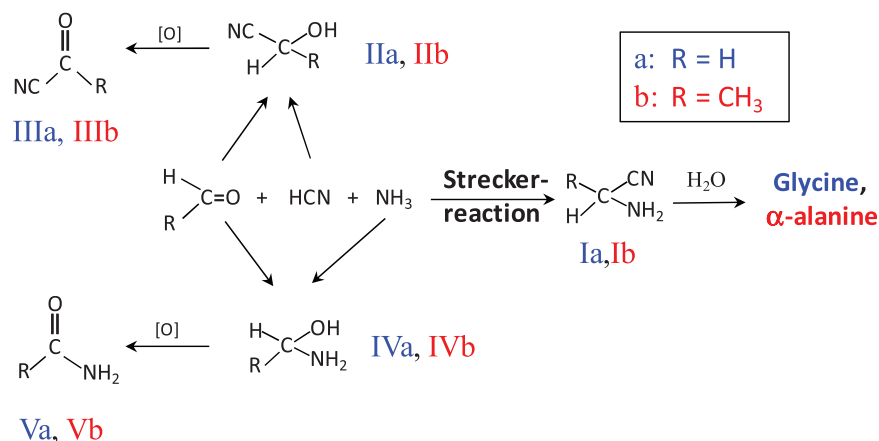
## I. INTRODUCTION

Recent substantial progress in astrophysical observation has permitted the detection of many, and more and more complex molecules in the interstellar medium (ISM) and in circumstellar envelopes. Observed molecules can be used as sensitive indicators to probe astrophysical processes such as accretion of matter in young stellar objects or plasma jets, for example. Complex chemical species give us insight, for instance, into the relationship between molecular clouds and planetary formation systems embedded in these clouds. The utility of molecules comes from both their spectra, which are highly instructive, and the chemical network they constitute. To date, more than 160 different molecules have been detected and 1/3 of them contain more than 6 atoms.<sup>1</sup> Most of these molecular identifications were accomplished after comparison of laboratory spectra to observations of interstellar surveys.

Of particular interest for astrobiology and the study of prebiotic chemistry in space are the recent detections of acetamide ( $\text{CH}_3\text{C}(\text{O})\text{NH}_2$ , see Ref. 2), the biggest molecule having a peptide-like bond, and aminoacetonitrile ( $\text{H}_2\text{NCH}_2\text{CN}$ , see Ref. 3) which is a direct precursor of glycine. The amino acid glycine can be formed from  $\text{H}_2\text{NCH}_2\text{CN}$  by simple hydrolysis. Especially, the presence of aminoacetonitrile in interstellar space strongly suggests that the Strecker reaction (cf. SCHEME 1), i.e., the reaction between an aldehyde, HCN, and  $\text{NH}_3$  (see Refs. 4(a),(b) and Scheme 1) actually occurs in the ISM. Indeed, this reaction and related pathways are thought to be a realistic and solid scenario for the formation of compounds like  $\text{H}_2\text{NCH}_2\text{CN}$  and other prebiotic nitriles in the ISM.<sup>5,6</sup> Some of the chemical compounds given in scheme 1 were already detected in the ISM, such as formamide (species Va, see, for example, Ref. 7 for the detection), acetamide (Vb, Ref. 2), aminoacetonitrile (Ia, Ref. 3), and also formyl cyanide which is species IIIa in scheme 1.<sup>8</sup> Others are expected to exist under interstellar conditions. Nevertheless, several molecular compounds involved in scheme 1 are still not well characterized in laboratory for their definitive identification in interstellar media. Furthermore, in order to model correctly the survival and evolution of such molecules in astrophysical objects, one needs reliable UV and vacuum ultraviolet (VUV) photophysical data and product branching ratios of photoreaction pathways.

At present, we studied the single-photon photoionization and dissociative photoionization spectroscopy of gas-phase acetyl cyanide ( $\text{H}_3\text{CC}(\text{O})\text{CN}$ ), species IIIb ( $\text{R} = \text{CH}_3$ ) in

<sup>a)</sup> Author to whom correspondence should be addressed. Electronic addresses: hochlaf@univ-mlv.fr, Tel.: +33160957319, Fax: +33160957320 and martin.schwell@lisa.u-pec.fr, Tel.: 0145171521.



SCHEME 1. Reactions and related pathways to be expected under interstellar conditions. Ia, IIIa, Va, and Vb compounds are actually observed. Others are expected to be present in the ISM.

scheme 1, by means of VUV synchrotron radiation (SR) and *ab initio* quantum chemistry methodologies. This molecule, denoted “AC” in this article (and sometimes called pyruvionitrile), could be formed by the photochemical hydrolysis of cyanoacetylene, or via the addition of HCN on acetaldehyde followed by an oxidation or by the reaction of the cyano and acetyl radicals on a grain. The former reaction is inspired from the Strecker scheme but with only two reagents R-CHO and HCN, and thus to form the corresponding cyanohydrin. The acetyl radical has already been proposed in the formation of several compounds detected in the ISM like acetaldehyde, acetone, acetic acid, methyl acetate, and the cyano radical in the formation of cyanopolynes and other nitriles. So far, AC is not detected in the ISM but, based on the arguments presented above, it is expected to exist there. Note also that its homologue IIIa was already observed in the ISM.<sup>8</sup>

Generally, the photophysics of AC has been studied widely in the mid-UV, essentially using laser based experiments. On the contrary, VUV photophysical data beyond the ionization energy (IE) of AC are scarce. Horwitz *et al.* studied its photofragmentation at  $\lambda = 193$  nm excitation using laser induced fluorescence (LIF) spectroscopy.<sup>9</sup> At this excitation wavelength, the  $S_3$  state of AC is populated and the molecule photodissociates into  $\text{CH}_3\text{CO} + \text{CN}$ , with the CN radical being formed in its electronic ground state  $X^2\Sigma^+$ . Shortly after this work, ultrafast pump probe spectroscopy in connection with quadrupole mass spectrometry has been used at the same excitation wavelength of  $\lambda = 193$  nm.<sup>10</sup> Products are probed using resonant two-photon ionization. The primary photoreaction  $\text{AC} + h\nu \rightarrow \text{CH}_3\text{CO} + \text{CN}$  is given to occur on a time scale of below 200 fs. The subsequent decomposition of the primary photoproduct  $\text{CH}_3\text{CO}$  is also observed with a 390 fs decay time. This decay time is interpreted there using Rice–Ramsperger–Kassel–Marcus theory. Photodissociation at  $\lambda = 193$  nm was further studied by Lee *et al.*<sup>11(a),11(b)</sup> In 2004, Aoyama *et al.*<sup>12</sup> used resonance enhanced multiphoton excitation at  $\lambda = 292$  nm. The nascent photofragment CN is formed in excited states  $A^2\Pi_1$  and  $B^2\Sigma^+$  when resonantly absorbing two of the 292 nm photons. The dispersed fluorescence of these states is observed experimentally and thoroughly interpreted. The first single photon VUV absorption spectrum is also presented by Aoyama *et al.*,<sup>12</sup> recorded using SR be-

tween 110 and 230 nm. In this spectrum, valence and Rydberg transitions, converging to the first ionization energy at 11.21 eV,<sup>13</sup> are identified. For the sake of completeness, we mention a matrix isolation study<sup>14</sup> where AC is trapped in an argon matrix and irradiated at wavelengths of either  $\lambda > 180$  or  $\lambda > 230$  nm. Several products are identified in matrix by IR spectroscopy, among them acetyl isocyanide  $\text{CH}_3\text{C(O)NC}$ , ketene:HCN and ketene:HNC complexes, as well as methyl cyanide ( $\text{CH}_3\text{CN}$ ) and methyl isocyanide ( $\text{CH}_3\text{NC}$ ).

Concerning the AC cation, insights on its ground state structure and its valence electronic states were detailed in the combined HeI photoelectron (PE) spectroscopic and theoretical study by Katsumata *et al.*<sup>13</sup> in the year 2000. Their PE spectrum extends up to 19 eV and consists of large bands which were assigned with the help of MP2/6-31G(d) and G3 calculations. In total, eight electronic cation states were attributed. To our knowledge, there is no photoionization mass spectrometric study of AC so far in the literature, treating photoexcitation in the spectral domain beyond the ionization energy of AC. Consequently, there is no information relative to the unimolecular decomposition processes of the  $\text{AC}^+$  ion formed upon photoionization of neutral AC.

In our work, the Photoelectron Photoion Coincidence (PEPICO) spectra of the monomer and of the lowest fragmentation channels, corresponding to the CN and CO loss reactions, are recorded. Since the main aim of this work is to give insight into the stability and reactivity of AC under interstellar conditions, we limited our spectra to  $h\nu < 13.6$  eV. This photon energy domain corresponds to interstellar “HI” regions where atomic hydrogen is not ionized. Photons with higher energy are effectively absorbed by atomic hydrogen in these regions and thus small and medium sized organic molecules may be protected from rapid destruction.

The interpretation of the experimental spectra was done with the help of quantum chemical calculations. We characterized the ground potential energy surfaces (PESs) of neutral acetyl cyanide and of its cation. These computations were carried out using both standard *ab initio* approaches (MP2 and coupled clusters) and the recently implemented explicitly correlated coupled clusters ((R)CCSD(T)-F12) technique. Therefore, we characterized the stable forms of the parent, the transition states connecting these minimal structures and the

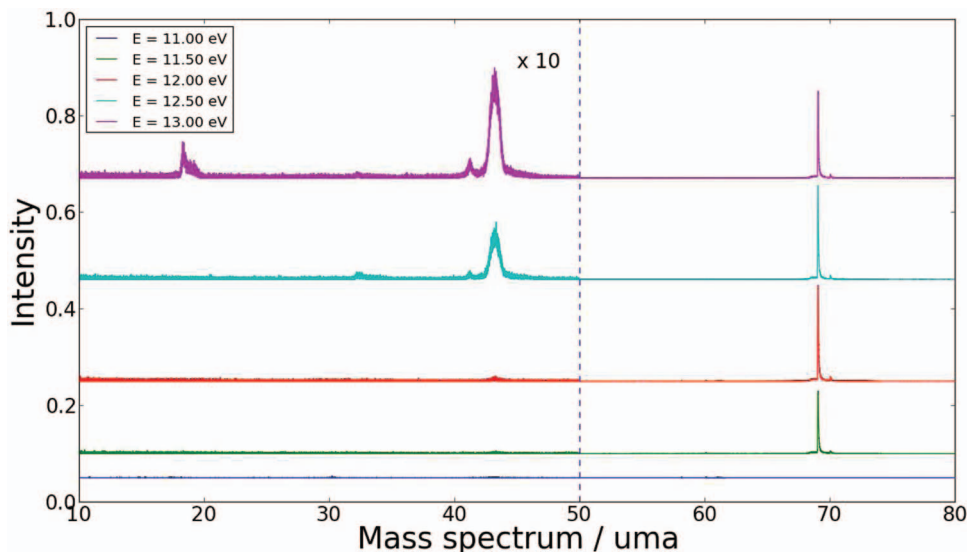


FIG. 1. TOF spectra recorded at 11, 11.5, 12, 12.5, and 13 eV photon energies (from bottom to top). The range of the Y axis is the same for all spectra. For amu <50, the signal is amplified by a factor of 10. The peak at 18 amu is due to residual water.

corresponding fragmentation pathways. We deduced hence the IEs of acetyl cyanide and the appearance energies (AEs) of the ionic fragments associated with CN, CO, and HCN loss channels.

## II. METHODOLOGIES

### A. Experimental

Our experiments were carried out at the DESIRS beamline of the French synchrotron facility SOLEIL<sup>15</sup> in con-

nection with its 6.65 m normal incidence monochromator and the photoion photoelectron coincidence spectrometer DELICIOUS III.<sup>16</sup> Briefly, this spectrometer allows for velocity map imaging of ions and electrons at the same time. The direction of ion/electron collection is perpendicular with respect to the molecular beam inlet and the VUV light propagation direction (all 90° setup). More details on the experimental setup can be found in Ref. 16. For our measurements, we used the 200 gr/mm grating of the monochromator with entrance/exit slit widths of typically 100/100 μm yielding a

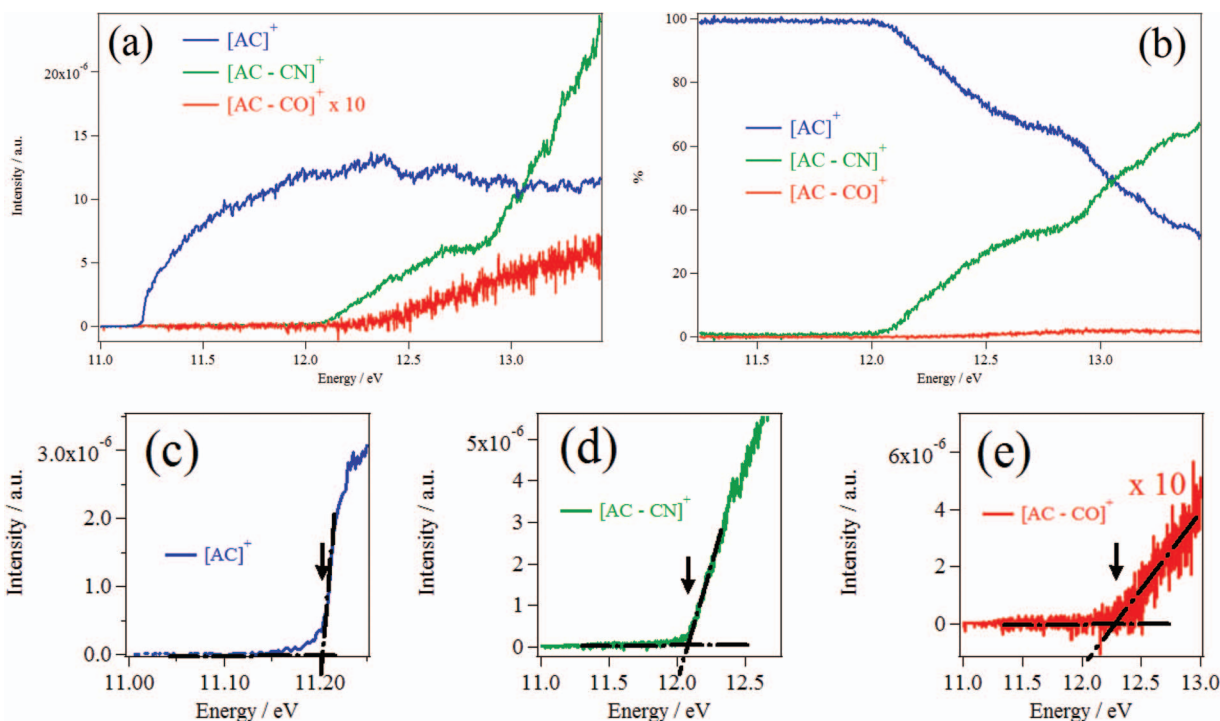


FIG. 2. In (a) PEPICO spectra as a function of the photon energy in the 11–13.5 eV range for  $\text{AC}^+$ ,  $[\text{AC}-\text{CO}]^+$  and  $[\text{AC}-\text{CN}]^+$ . The  $[\text{AC}-\text{CO}]^+$  signal is very low and it was amplified by a factor of 10. In (b), breakdown diagram in the 11–13.5 eV energy range. At each energy, the sum of three contributions is 100%. Traces (c), (d), and (e) are enlargements in the regions of the IE and AEs. The measured values are noted by vertical arrows. The energies are given with respect to neutral AC ground state.

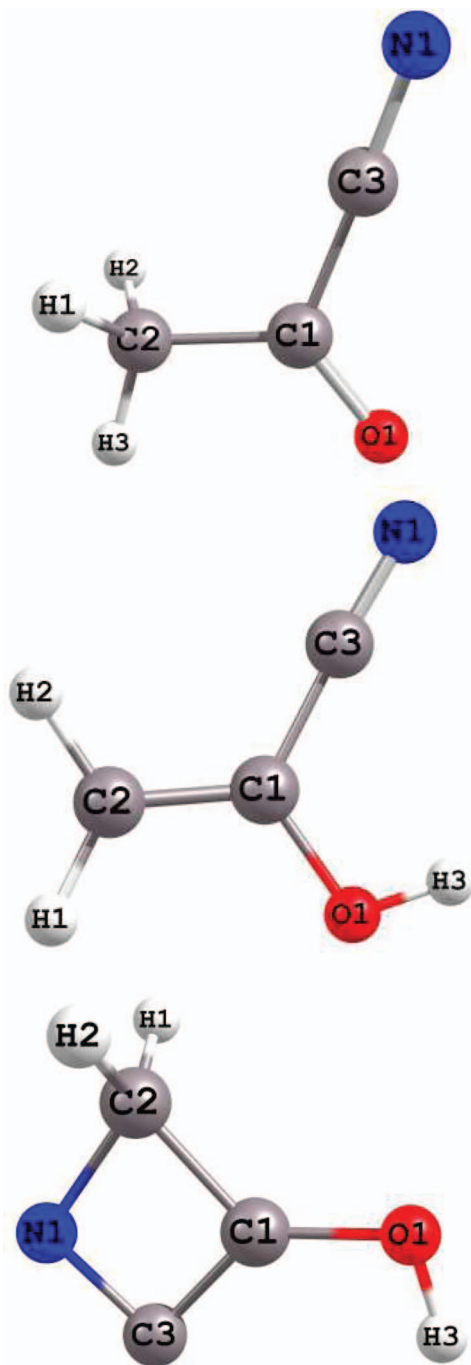


FIG. 3. Optimized structures of neutral and cationic acetyl cyanide and of their tautomers. The numbering of the atoms used in Table I is also given. The upper trace is for AC keto structures, middle trace is for enol forms and lower trace for TS1 and TS1<sup>+</sup>. See Figure 4 for the denomination of the molecular species under consideration.

spectral resolution (photons) of 0.72 Å. We collected all photoelectrons having kinetic energies less than 3.5 eV in coincidence with the corresponding photoions.

The PEPICO spectra are further normalized by the photon flux measured by a photodiode (AXUV, IRD) which is placed after the photoionization region. For better spectral purity, we use the gas filter of the beamline which is filled with 0.25 mbar of Ar. This allows for effective suppression of

higher energy stray light of the electron storage ring, as well as higher order radiation of the undulator.<sup>17</sup>

AC is purchased from Sigma-Aldrich (stated purity  $\geq 90\%$ ). No further purification is done since the PEPICO technique implemented in DELICIOUS III allows for species selective spectroscopy. The sample is placed in a bubbler flask at room temperature. This flask is connected directly to the molecular beam chamber which is attached to the DELICIOUS III spectrometer. The vapor pressure of AC is such that no carrier gas is needed to drain the pure compound through the 50  $\mu\text{m}$  nozzle expansion and skimmer towards the ionization region.

## B. Computational

All computations were performed with MOLPRO (version 2012) package.<sup>18</sup> They consist of geometry optimizations of the molecular structures (both neutral and ionic), as well as the harmonic frequencies calculations to attest on the nature of the stationary points found (either a minimum or a transition state). These calculations were done in the C<sub>1</sub> point group using the default options as implemented in MOLPRO. Here, the C, H, N, and O atoms were described using the aug-cc-pVXZ (X = D,T,Q) basis sets.<sup>19</sup>

Katsumata *et al.*<sup>13</sup> showed that the ground state of neutral AC is of singlet spin multiplicity and that the cation is of doublet ground state. Both of them are described by a dominant electron configuration, validating hence the use of mono configurational approaches for the treatment of these species. Hence, the stationary points on the ground potential energy surface of AC and of AC<sup>+</sup> were characterized first at the Møller Plesset (R)MP2/aug-cc-pVTZ level of theory.<sup>20</sup>

For better accuracy, explicitly correlated computations (cf. Refs. 21(a)–(c)) at the (R)CCSD(T)-F12/aug-cc-pVDZ (approximation b) level were done, where we followed the methodology described in Ref. 22. Briefly, the C, H, N, and O atoms were described using the aug-cc-pVTZ basis sets, in connection with the corresponding auxiliary basis sets and density fitting functions, where the default CABS(OptRI) basis sets were used.<sup>23(a),23(b),23(c),23(d)</sup>

We performed also single point computations on the optimized structures using the standard coupled cluster approach with perturbative treatment of triple excitations<sup>24(a),24(b)</sup> in connection with the aug-cc-pVQZ basis set (i.e., (R)CCSD(T)/aug-cc-pVQZ level) and the explicitly correlated coupled cluster (approximation b) where the atoms were described by the aug-cc-pVTZ basis set (i.e., (R)CCSD(T)-F12/aug-cc-pVTZ level). This allows for getting more accurate energetics.

## III. PEPICO SPECTRA

### A. Time of flight (TOF) spectra

Figure 1 presents TOF mass spectra (TOF MS) of AC at fixed photon energies from 11 to 13 eV by steps of 0.5 eV. Below 11 eV, the TOF MS shows close to zero signal since these photon energies are below the adiabatic ionization energy (AIE) of AC (found at 11.21 eV by Katsumata *et al.*<sup>13</sup>).

TABLE I. Main geometrical parameters (Å and degrees) of neutral and cationic acetyl cyanide and of its tautomer obtained at (R)CCSD(T)-F12/aug-cc-pVDZ level of theory. See Figure 3 for the definition of the structures and the numbering of the atoms. All species belong to  $C_s$  point group.

	AC ( $\bar{X}^1A'$ )	TS1 ( $\bar{X}^1A'$ )	AC-ol MIN1 ( $\bar{X}^1A'$ )	TS2 ( $\bar{X}^1A'$ )	AC-ol MIN2 ( $\bar{X}^1A'$ )	AC <sup>+</sup> ( $\bar{X}^2A'$ )	TS1 <sup>+</sup> ( $\bar{X}^2A'$ )	AC-ol <sup>+</sup> MIN1 ( $\bar{X}^2A''$ ) <sup>a</sup>	TS2 <sup>+</sup> ( $\bar{X}^2A'$ )	AC-ol <sup>+</sup> MIN2 ( $\bar{X}^2A''$ ) <sup>a</sup>
C <sub>1</sub> -C <sub>2</sub>	1.49	1.48	1.33	1.37	1.33	1.46	1.49	1.41	1.44	1.42
C <sub>1</sub> -C <sub>3</sub>	1.47	1.44	1.43	1.47	1.43	1.44	1.48	1.44	1.43	1.44
C <sub>3</sub> -N	1.17	1.37	1.17	1.17	1.17	1.12	1.21	1.13	1.17	1.12
C <sub>1</sub> -O	1.21	1.29	1.36	1.31	1.36	1.23	1.24	1.27	1.27	1.27
C <sub>2</sub> -H <sub>1</sub>	1.09	1.08	1.07	1.10	1.08	1.09	1.08	1.08	1.08	1.08
C <sub>2</sub> -H <sub>2</sub>	1.09	1.08	1.07	1.10	1.07	1.09	1.08	1.08	1.08	1.08
C <sub>2</sub> -H <sub>3</sub>	1.08	...	...	...	...	1.08	...	...	...	...
O-H <sub>3</sub>	...	0.97	0.96	0.97	0.96	...	0.98	0.98	0.98	0.98
N-C <sub>3</sub> -C <sub>1</sub>	178.8	86.36	176.9	170.2	179.0	177.8	95.9	177.9	179.0	177.6
C <sub>3</sub> -C <sub>1</sub> -O	119.8	133.34	116.3	112.43	111.8	113.0	139.3	118.3	118.9	113.7
O-C <sub>1</sub> -C <sub>2</sub>	125.4	130.24	121.8	121.6	126.9	121.9	133.7	117.4	118.7	123.6
C <sub>1</sub> -C <sub>2</sub> -H <sub>3</sub>	109.7	...	...	...	...	112.3	...	...	...	...
C <sub>1</sub> -C <sub>2</sub> -H <sub>1</sub>	109.3	116.9	120.1	106.4	121.1	106.1	116.1	119.6	118.9	120.1
C <sub>1</sub> -C <sub>2</sub> -H <sub>2</sub>	109.3	116.9	119.4	106.4	119.5	106.1	116.1	118.5	118.9	119.2

<sup>a</sup>RMP2/aug-cc-pVTZ level.

The TOF mass spectra at 11.5 and 12 eV are dominated by a peak at  $m/z$  69 corresponding to the AC<sup>+</sup> parent ion. For  $h\nu \geq 12.5$  eV, two different masses lighter than AC<sup>+</sup> are observed (at  $m/z$  41 and 43). *A priori*, the first one corresponds to an ion formed by CO loss and the second to an ion formed by CN loss from the AC<sup>+</sup> cation. Both fragments originate from AC<sup>+</sup> parent as checked by our analysis of their kinetic energy releases, which are above the expected thermal energies. Indeed, the width of the fragments peaks is significantly larger than the parent one.

The fragment ions formed by dissociative photoionization are denoted hereafter as [AC-CO]<sup>+</sup> and [AC-CN]<sup>+</sup>. We note that the parent ion of acetic acid, which could be a potential impurity in the commercial sample formed by hydrolysis, at  $m/z$  60 is not observed. Therefore, we expect no contribution to the  $m/z$  43 signal from dissociative ionization of acetic acid. The latter has been observed by Leach *et al.*<sup>25</sup>

## B. PEPICO photoionization efficiency (PIE) spectra

Figure 2 displays the PEPICO PIE spectra of AC<sup>+</sup> ( $m/z$  69) and of the two ionic fragments [AC-CO]<sup>+</sup> ( $m/z$  41) and [AC-CN]<sup>+</sup> ( $m/z$  43) in the 11-13.5 eV photon energy range. The signal associated to [AC-CO]<sup>+</sup> is relatively weak (as can already be noticed in the mass spectra). It is therefore magnified by a factor of 10 in Figure 2. In addition, Figure 2(b) shows branching ratios of formation of each of the 3 ions as a function of energy.

Below 11 eV, no signal is recorded (cf. TOF MS in Figure 1). The spectrum of AC<sup>+</sup> consists on a sharp onset at  $h\nu \sim 11.2$  eV followed by a plateau for  $h\nu > 12$  eV. The sharp onset corresponds to the AIE of AC. Using linear extrapolation close to IE (Figure 2(c)), we deduce AIE(AC) =  $11.20 \pm 0.01$  eV. This AIE agrees quite well with the unique available IE from the literature found at IE = 11.21 eV by Katsumata *et al.*<sup>13</sup> using HeI photoelectron spectroscopy. The value of 11.21 eV from Ref. 13 corresponds to the maximum of the intense  $0_0^0$  transition of the vibronic progression

of the first photoelectron spectrum band observed there. The 11.21 eV band is the most intense band of this progression and we therefore consider that the value of Katsumata *et al.*<sup>13</sup> corresponds to the vertical IE (VIE) of AC rather than AIE of AC. Both values are close in energy since the difference between the AIE and VIE is only of the order of 0.01 eV, which is close to our experimental accuracy. Therefore, one can expect only small geometry changes of the molecule upon ionization. These findings are supported by the calculations presented below.

The PEPICO PIE spectra of [AC-CO]<sup>+</sup> and [AC-CN]<sup>+</sup> fragment ions both show a smooth increase of the signal at their respective AE thresholds. We measure AE([AC-CO]<sup>+</sup>) =  $12.29 \pm 0.01$  eV and AE([AC-CN]<sup>+</sup>) =  $12.07 \pm 0.01$  eV by linear extrapolation of the onset signal to zero (Figures 2(d) and 2(e)). In the literature, there are no available data on these quantities to compare with. We also present in Figure 2 the breakdown diagram of AC in the 11–13.5 eV energy range.

## IV. GROUND STATE POTENTIAL OF ACETYL CYANIDE AND OF ITS CATION

The main aim of the present computations is to provide interpretation of the experimental spectra. For that purpose, we mapped the PESs of AC and of its cation. These PESs cover the equilibrium structures, the transition states, and the lowest cationic fragmentation channel regions. In the following, we will discuss the (R)CCSD(T)-F12/aug-cc-pVDZ values.

Figure 3 shows the optimized structures of AC and AC<sup>+</sup>. The corresponding geometrical parameters are listed in Table I. Figure 4 displays the ground state PESs of AC and of AC<sup>+</sup>. For neutral AC, we found two transition states (TS1 and TS2) and two equilibrium structures corresponding to the enol forms (AC-ol MIN1 and AC-ol MIN2) in addition to the keto form already characterized by Katsumata *et al.*<sup>13</sup> TS1 connects the keto and the enol isomers. At the CCSD(T)-F12/aug-cc-pVDZ level, TS1 is located at  $\sim 4.4$  eV with

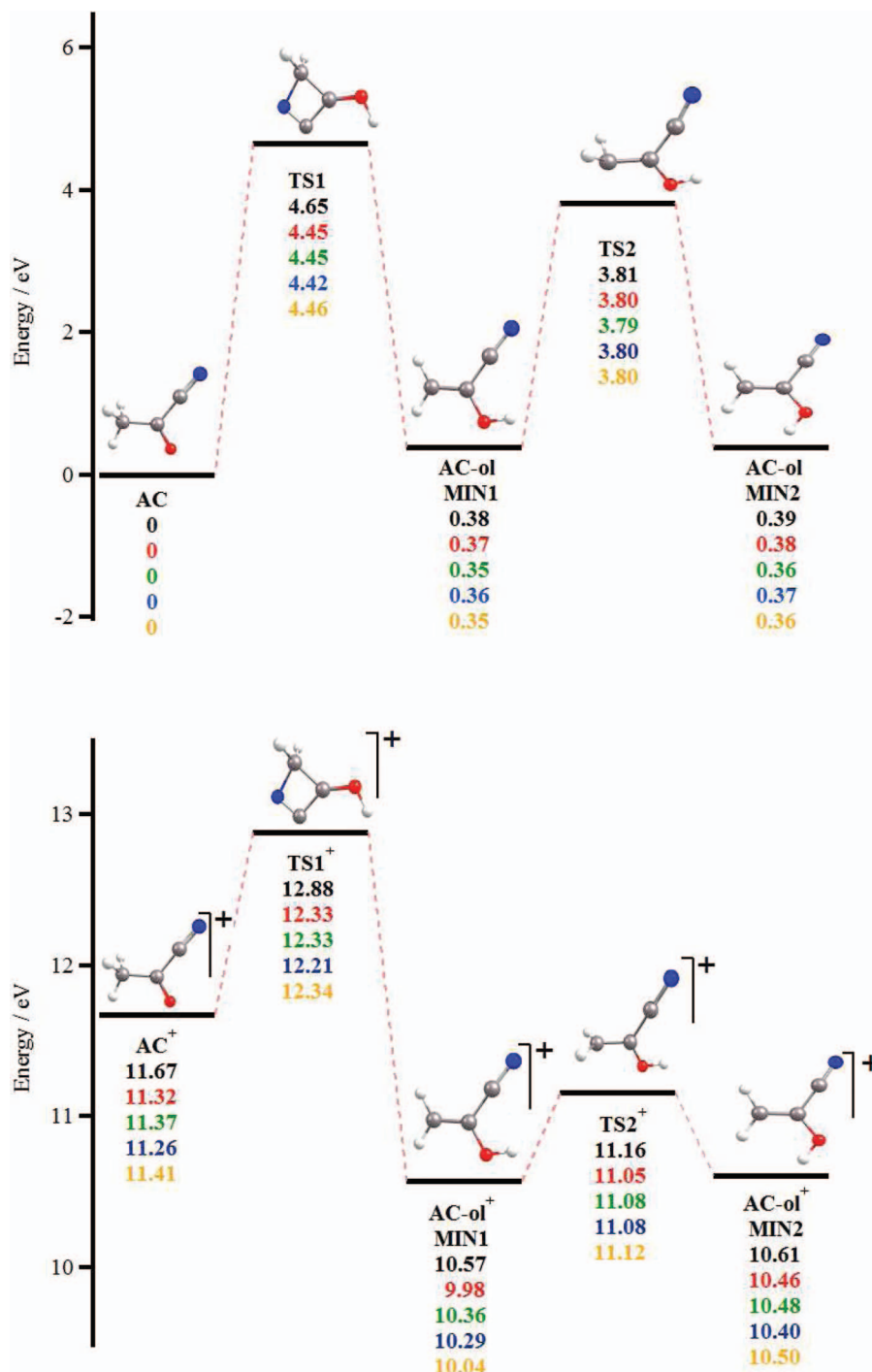


FIG. 4. Potential energy surfaces (PESs) of neutral (upper trace) and ionic (lower trace) AC. The energies in black, red, green, blue, and yellow are those computed at (R)MP2/aug-cc-pVTZ (Opt), (R)CCSD(T)/aug-cc-pVTZ (SP), (R)CCSDT(T)/aug-cc-pVQZ (SP), (R)CCSDT(T)-F12/aug-cc-pVDZ (Opt), (R)CCSDT(T)-F12/aug-cc-pVTZ (SP) levels, respectively. Opt is when full geometry optimizations are performed and SP is for single point computations (see text). The energies are given with respect to neutral AC ground state minimum energy.

respect to the keto form. AC-ol MIN1 and AC-ol MIN2 are located at  $\sim 0.36$  eV. Both species are separated by a potential barrier of  $\sim 3.80$  eV where one can find TS2. We may convert AC-ol MIN1 into AC-ol MIN2 after rotation of the OH distance along the CO bond. A potential barrier of  $\sim 0.21$  eV is computed between both conformers.

Similar to the neutral species, the cation possesses a keto form (AC<sup>+</sup>), two minimal structures for the enol forms (AC-ol<sup>+</sup> MIN1 and AC-ol<sup>+</sup> MIN2) and two transition states (TS1<sup>+</sup>

and TS2<sup>+</sup>). For the cation, enol isomers are more stable than the keto form (by  $\sim 1$  eV). AC<sup>+</sup> converts by intramolecular proton transfer into the enol forms via TS1<sup>+</sup> by proton transfer from N<sub>1</sub> to O<sub>1</sub> (Figure 3). The potential barrier for this conversion is computed  $\sim 1$  eV with respect to AC<sup>+</sup>. AC-ol<sup>+</sup> MIN1 and AC-ol<sup>+</sup> MIN2 are separated by a potential barrier of  $\sim 0.7$  eV where we located TS2<sup>+</sup>. Both conformers convert after rotating the OH around the CO bond (potential barrier of  $\sim 0.8$  eV). We also investigated the AC<sup>+</sup> decarbonylation

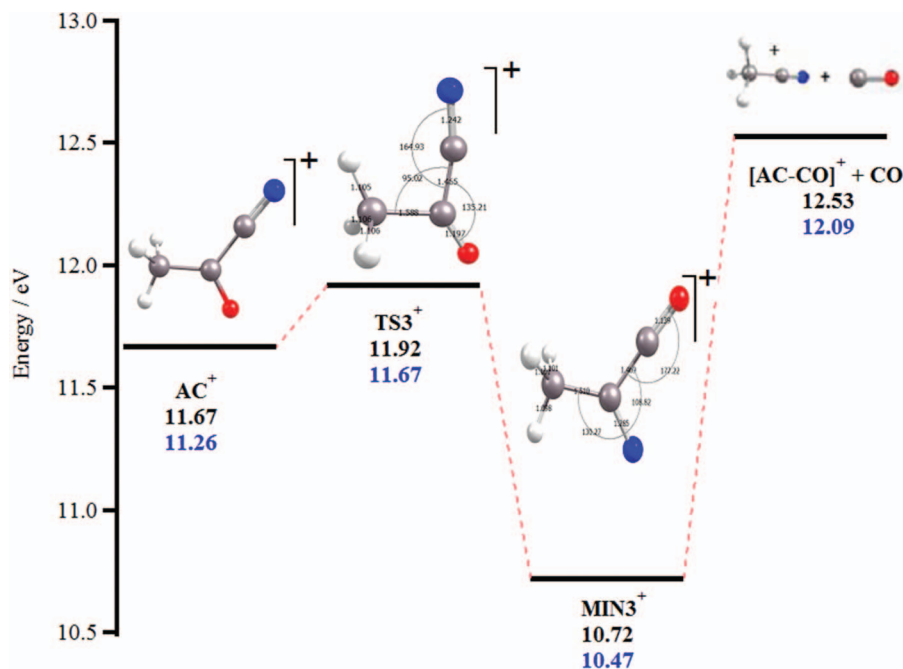


FIG. 5. The energy profile for the decarbonylation from the  $AC^+$  cation computed at the RMP2/aug-cc-pVTZ (in black) level of theory. We also give the main geometrical parameter of  $TS3^+$  and of  $MIN3^+$  (distances in Å and angles in degrees). The energies in blue are those computed at the (R)CCSD(T)/aug-cc-pVDZ level. The energies are given with respect to neutral AC ground state minimum energy.

reaction pathway where an additional transition state and a minimal structure are found (denoted as  $MIN3^+$  and  $TS3^+$ , Figure 5).

The geometries of the stationary points on PESs of AC and  $AC^+$  are listed in Table I. Upon ionization, there are no strong changes in the equilibrium geometries. For neutral AC, our computed geometry is close to the one calculated earlier by Katsumata *et al.*<sup>13</sup> Table II lists the lowest dissociation limits of  $AC^+$ . We give also the theoretically computed AEs, which are given relative to the AC ground state. We were looking for fragments either neutral or positively charged in their lowest spin multiplicities (doublet or quartet and singlet or triplet). Our computations show that the lowest dissociation limit of  $AC^+$  corresponds to the dissociative ionization reaction  $AC^+ \rightarrow HCN + O = C-CH_2^+$  appearing at  $\sim 10.7$  eV (mass peak  $m/z$  42). It is followed by the  $AC^+ \rightarrow CO + CH_3-CN^+$  (mass peak at  $m/z$  41) channel at 12.09 eV. The energy of the  $AC^+ \rightarrow CN + CH_3-CO^+$  (mass peak at  $m/z$  43) is computed  $\sim 12.25$  eV.

For the  $HCN + O = C-CH_2^+$  fragmentation channel, we also computed the dissociation limits associated with electronically excited  $O = C-CH_2^+$ . They are located at  $\sim 11.4$  eV and at  $\sim 13.0$  eV, where the ion is either in its electronic ground or excited state. The corresponding vertical excitation energy was calculated using the state-averaged complete active space self-consistent field (CASSCF)<sup>26</sup> method and the aug-cc-pVTZ basis set. The upper dissociation limits are located above 13.5 eV (see Table II for more details).

## V. DISCUSSION

Our computations reveal that the keto and enol forms of neutral AC are separated by large potential barriers. So at room temperature, the molecular beam is composed solely

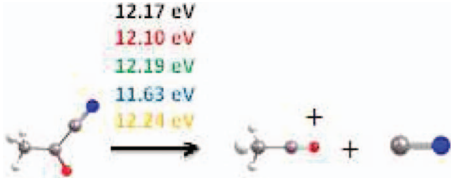
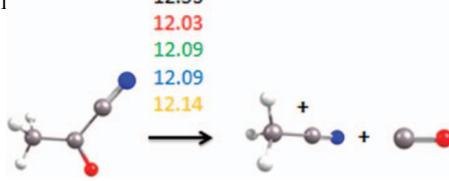
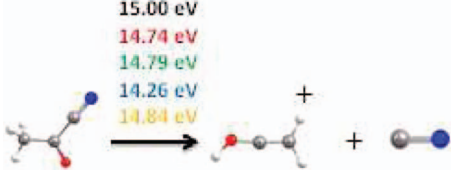
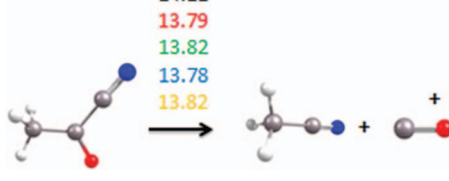
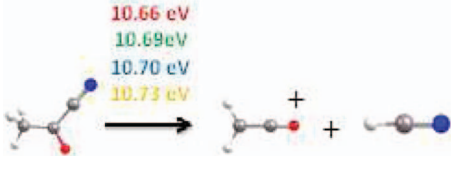

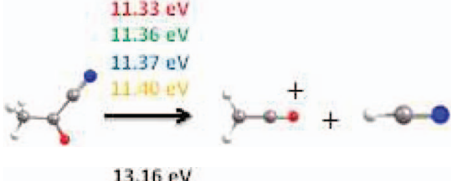
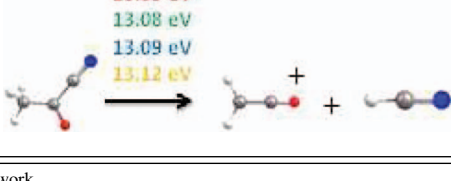
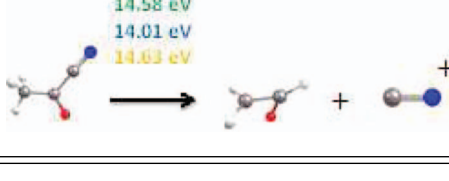
by the keto form. Moreover, Table I shows that AC and  $AC^+$  have close equilibrium geometries. Accordingly, we populate preferentially the  $AC^+$  isomer upon single photoionization. We give in Figure 4 the adiabatic ionization energies of AC and of the enol forms of AC with respect to the AC ground state. Note that all levels of theory lead to sensitively similar results. Especially, (R)CCSD(T)/aug-cc-pVQZ (green) and (R)CCSD(T)-F12/aug-cc-pVTZ (yellow) give similar results whereas the computational cost of the explicitly correlated method (both CPU and disk space) is reduced by up to two orders of magnitude. Therefore, (R)CCSD(T)-F12/aug-cc-pVDZ (blue) is recommended for the computations of properties of medium sized prebiotic molecules. At this level of theory, we compute  $IE(AC) = 11.26$  eV. The theoretical  $IE(AC)$  agrees well with the present and previous experimental IEs. This attests on the high accuracy of the present theoretical determinations.

Upon formation,  $AC^+$  undergoes two fragmentation pathways. The first one is obvious and leads to the formation to the CN and  $H_3C-CO^+$  cation. The experimental AE of  $H_3C-CO^+$  is measured AE ( $[AC-CN]^+$ ) =  $12.07 \pm 0.01$  eV which is in close agreement with the computed value of  $\sim 12.25$  eV. This fragmentation most likely occurs via CC bond breaking between the  $CH_3CO$  and the cyano group of  $AC^+$ .

The second observed fragmentation is associated with the production of CO and the  $CH_3CN^+$  ion. We measure  $AE([AC-CO]^+) = 12.29 \pm 0.01$  eV which is close to the calculated AE at  $\sim 12.09$  eV. Figure 5 shows that the  $AC^+ \rightarrow [AC-CO]^+ + CO$  reaction occurs through  $TS3^+$ , where  $MIN3^+$  ions are formed intermediately. Then  $MIN3^+$  ions dissociate to form the corresponding products. Such mechanism was observed already for other ionized prebiotic molecules (e.g., 2-pyridone<sup>+</sup>/2-hydroxypyridine<sup>+</sup>,<sup>27</sup>



TABLE II. Experimental linear extrapolated appearance energies ( $AE_{\text{exp}}$ ) of the masses observed in the dissociative photoionization of AC, along with their calculated fragmentation pathways. The energies in black, red, green, blue, and yellow are those computed at (R)MP2/aug-cc-pVTZ (Opt), (R)CCSD(T)/aug-cc-pVTZ (SP), (R)CCSDT(T)/aug-cc-pVQZ (SP), (R)CCSDT(T)-F12/aug-cc-pVDZ (Opt), (R)CCSDT(T)-F12/aug-cc-pVTZ (SP) levels, respectively. Opt is when full geometry optimizations are performed and SP is for single point computations (see text).

Mass (amu)	$AE_{\text{exp}}$ (eV)	Calculated channel	Mass (amu)	$AE_{\text{exp}}$ (eV)	Calculated channel
43	$12.07 \pm 0.01$		41	$12.29 \pm 0.01$	
			28	...	
42	...		27	...	
					
			26	...	

<sup>a</sup>Not measured in the present work.

<sup>b</sup>We added the electronic excitation energies of  $O = C-CH_2^+$  to the computed energies for the ground state.

$\delta$ -valerolactam<sup>+28</sup>) and DNA bases (such as thymine<sup>+</sup> and cytosine<sup>+</sup> radical cations<sup>29</sup>).

TS3<sup>+</sup> is located slightly higher in energy than AC<sup>+</sup> (by  $\sim 0.25$  eV). At the RCCSD(T)/aug-cc-pVDZ, TS3<sup>+</sup> is located at  $\sim 11.67$  eV which is distinctly lower than that the computed and measured  $AE([AC-CO]^+)$ . This suggests that the formation of  $CO + CH_3CN^+$  after AC VUV photon absorption takes place via a complex mechanism: The ejection of CO is most likely associated with rearrangements before ionization leading to the formation of CC bond between the  $CH_3$  and the CN moieties. Alternatively, we populate the dissociative excited states of AC<sup>+</sup> that lead to the corresponding products.

Theoretically, the lowest dissociation limit corresponds to the formation of  $HCN (+CH_2CO^+)$  at 10.7 eV. Electronically excited  $CH_2CO^+$  ions are also expected to be formed. Despite that these channels are the most thermodynamically favorable channels, they are not observed experimentally.

This is probably because of the predominance of the two other channels as can be seen in the breakdown diagram of Figure 2(b).

Note that the mid-UV and VUV photodissociation below the IE of AC produces  $CH_3 + COCN$  (this is a minor channel however) and  $CN + CH_3CO$  fragments (main channel). These two fragmentation channels result from two different C–C bond cleavages (see, for example, Refs. 9, 10, and 12). Below the IE, there is no evidence from the literature for the formation of CO as evidenced here for AC<sup>+</sup>. This is a signature of new and different chemistry occurring upon ionization.

## VI. GENERAL COMMENTS AND ASTROPHYSICAL IMPLICATIONS

We presented a combined theoretical and experimental work dealing with the photoionization and dissociative photoionization of AC in gas phase. Accurate thermochemical

data were deduced. Moreover, we show that the energy ordering of the organic tautomers is reversed upon ionization. In addition, new and complicated chemistry under ionizing conditions is viewed to be in action. Indeed, we found that the unimolecular ionic fragmentation pathways may depend on the skeletal molecular structure via the involvement of several isomeric forms of the intermediate species. The present findings should be incorporated into the astrophysical models dedicated to the characterization of the ISM and of its physico-chemical composition and evolution.

The interpretation and assignment of the experimental findings requires state-to-the-art theoretical methodologies. In this context, the newly implemented explicitly correlated methods are viewed to provide accurate data with reduced computational cost.<sup>30(a),30(b)</sup> From a perspective point of view, our work shows that photoelectron spectra of organic medium sized molecules may have different contributions associated with different photoionization and dissociative ionization processes, which are worth to investigate by means of the emerging photoelectron spectroscopies such as slow photoelectron spectroscopy.<sup>31(a),31(b),31(c)</sup>

## ACKNOWLEDGMENTS

We would like to thank Gustavo Garcia, Laurent Nahon, and Jean-François Gil for excellent support and working conditions at the DESIRS beamline at Soleil. We are also indebted to the general technical staff of Synchrotron Soleil for the running the facility. M.H., M.S., and J.-C.G. acknowledge the French National Program *Physique et Chimie du Milieu Interstellaire*, PCMI (INSU, CNRS) for financial support. M.H. and M.M.A. would like to extend their sincere appreciation to the Deanship of Scientific Research at King Saud University for its funding the research through the Research Group Project No. RGP-VPP-333.

<sup>1</sup>E. Herbst and E. F. van Dishoeck, *Annu. Rev. Astron. Astrophys.* **47**, 427 (2009).

<sup>2</sup>J. M. Hollis, F. J. Lovas, A. J. Remijan, P. R. Jewell, V. V. Iyushin, and I. Kleiner, *Astrophys. J.* **643**, L25 (2006).

<sup>3</sup>A. Belloche, K. M. Menten, C. Comito, H. S. P. Müller, P. Schilke, J. Ott, S. Thorwirth, and C. Hieret, *Astron. Astrophys.* **482**, 179 (2008).

<sup>4</sup>(a) A. Strecker and A. Ueber, *Annu. Chem. Pharm.* **75**, 27 (1850); (b) A. Strecker, *ibid.* **91**, 349 (1854).

<sup>5</sup>U. Meierhenrich, "Amino acids and the asymmetry of life," *Advances in Astrobiology and Biogeophysics* (Springer, Berlin, 2008).

<sup>6</sup>G. Danger, F. Borget, M. Chomat, F. Duvernay, P. Theulé, J. C. Guillemin, L. Le Sergeant d'Hendecourt, and T. Chiavassa, *Astron. Astrophys.* **535**, A47 (2011).

<sup>7</sup>C. Kahane, C. Ceccarelli, A. Faure, and E. Caux, *Astrophys. J.* **763**, L38 (2013).

<sup>8</sup>A. J. Remijan, J. M. Hollis, F. J. Lovas, W. D. Stork, P. R. Jewell, and S. D. Meier, *Astrophys. J.* **675**, L85–L88 (2008).

<sup>9</sup>R. J. Horwitz, J. S. Francisco, and J. A. Guest, *J. Phys. Chem. A* **101**, 1231 (1997).

<sup>10</sup>J. C. Owrutsky and A. P. Baronavski, *J. Chem. Phys.* **111**, 7329 (1999).

<sup>11</sup>(a) I. R. Lee, W. K. Chen, Y. C. Chung, and P. Y. Cheng, *J. Phys. Chem. A* **104**, 10595 (2000); (b) I. R. Lee, Y. C. Chung, W. K. Chen, X. P. Hong, and P. Y. Cheng, *J. Chem. Phys.* **115**, 10656 (2001).

<sup>12</sup>J. I. Aoyama, T. Sugihara, K. Tabayashi, and K. Saito, *J. Chem. Phys.* **118**, 6348 (2003).

<sup>13</sup>S. Katsumata, K. Tabayashi, T. Sugihara, and K. Kimura, *J. Electron Spectrosc. Relat. Phenom.* **113**, 49 (2000).

<sup>14</sup>Z. Guennoun, I. Couturier-Tamburelli, S. Combes, J. P. Aycard, and N. Piétri, *J. Phys. Chem. A* **109**, 11733 (2005).

<sup>15</sup>L. Nahon, N. de Oliveira, G. A. Garcia, J. F. Gil, B. Pilette, O. Marcouillé, B. Lagarde, and F. Polack, *J. Synchrotron Radiat.* **19**, 508 (2012).

<sup>16</sup>G. A. Garcia, B. K. Cunha de Miranda, M. Tia, S. Daly, and L. Nahon, *Rev. Sci. Instrum.* **84**, 053112 (2013).

<sup>17</sup>B. Mercier, M. Compin, C. Prevost, G. Bellec, R. Thissen, O. Dutuit, and L. Nahon, *J. Vac. Sci. Technol. A* **18**, 2533 (2000).

<sup>18</sup>H.-J. Werner, P. J. Knowles, G. Knizia, F. R. Manby, M. Schütz *et al.*, MOLPRO, version 2012.1, a package of *ab initio* programs, 2012, see <http://www.molpro.net>.

<sup>19</sup>T. H. Dunning, *J. Chem. Phys.* **90**, 1007 (1989); R. A. Kendall, T. H. Dunning, and R. J. Harrison, *ibid.* **96**, 6796 (1992).

<sup>20</sup>C. Møller and M. S. Plesset, *Phys. Rev.* **46**, 618 (1934).

<sup>21</sup>(a) T. B. Adler, G. Knizia, and H. J. Werner, *J. Chem. Phys.* **127**, 221106 (2007); (b) H. J. Werner, G. Knizia, and F. R. Manby, *Mol. Phys.* **109**, 407 (2011); (c) G. Knizia, T. B. Adler, and H. J. Werner, *J. Chem. Phys.* **130**, 054104 (2009).

<sup>22</sup>Y. Pan, K. C. Lau, M. M. Al-Mogren, A. Mahjoub, and M. Hochlaf, *Chem. Phys. Lett.* **613**, 29–33 (2014).

<sup>23</sup>(a) F. Weigend, *Phys. Chem. Chem. Phys.* **4**, 4285 (2002); (b) C. Hättig, *ibid.* **7**, 59 (2005); (c) W. Klopper, *Mol. Phys.* **99**, 481 (2001); (d) K. E. Yousaf and K. A. Peterson, *J. Chem. Phys.* **129**, 184108 (2008).

<sup>24</sup>(a) G. D. Purvis III and R. J. Bartlett, *J. Chem. Phys.* **76**, 1910 (1982); (b) C. Hampel, K. A. Peterson, and H. J. Werner, *Chem. Phys. Lett.* **190**, 1 (1992).

<sup>25</sup>S. Leach, M. Schwell, H. W. Jochims, and H. Baumgärtel, *Chem. Phys.* **321**, 171 (2006).

<sup>26</sup>P. J. Knowles and H. J. Werner, *Chem. Phys. Lett.* **115**, 259 (1985); H. J. Werner and P. J. Knowles, *J. Chem. Phys.* **82**, 5053 (1985).

<sup>27</sup>M. A. Trikoupi, P. Gerbaux, D. J. Lavorato, R. Flammang, and J. K. Terlouw, *Int. J. Mass Spectrom.* **217**, 1 (2002); J. C. Choe, *Bull. Korean Chem. Soc.* **35**, 3021 (2014).

<sup>28</sup>A. Mahjoub, M. Hochlaf, G. A. Garcia, L. Nahon, and L. Poisson, *J. Phys. Chem. A* **116**, 8706 (2012).

<sup>29</sup>H. W. Jochims, M. Schwell, H. Baumgärtel, and S. Leach, *Chem. Phys.* **314**, 263 (2005).

<sup>30</sup>(a) V. Brites and M. Hochlaf, *J. Phys. Chem. A* **113**, 11107 (2009); (b) H. J. Werner, G. Knizia, T. B. Adler, and O. Marchetti, *Z. Phys. Chem.* **224**, 493 (2010).

<sup>31</sup>(a) J. C. Pouilly, J. P. Schermann, N. Nieuwjaer, F. Lecomte, G. Grégoire, C. Desfrancois, G. A. Garcia, L. Nahon, D. Nandi, L. Poisson, and M. Hochlaf, *Phys. Chem. Chem. Phys.* **12**, 3566 (2010); (b) M. Briant, L. Poisson, M. Hochlaf, P. de Pujo, M. A. Gaveau, and B. Soep, *Phys. Rev. Lett.* **109**, 193401 (2012); (c) Y. Pan, K. C. Lau, L. Poisson, G. A. Garcia, L. Nahon, and M. Hochlaf, *J. Phys. Chem. A* **117**, 8095 (2013).